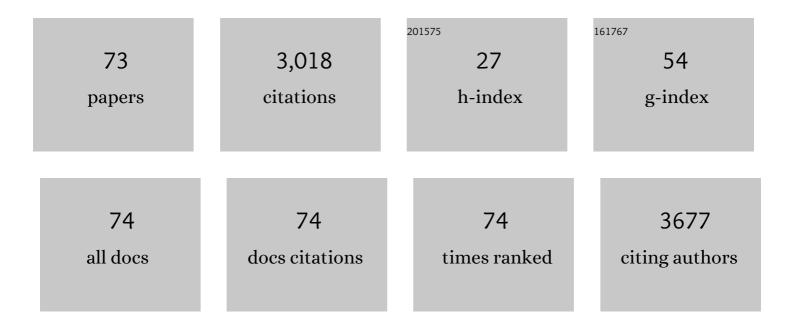
List of Publications by Year in descending order

Source: https://exaly.com/author-pdf/7608156/publications.pdf Version: 2024-02-01



Διοκ Κ Μιτρλ

#	Article	IF	CITATIONS
1	Structure and function of aquaporin water channels. American Journal of Physiology - Renal Physiology, 2000, 278, F13-F28.	1.3	558
2	Three-dimensional organization of a human water channel. Nature, 1997, 387, 627-630.	13.7	288
3	Membrane Structures in Normal and Essential Fatty Acid-Deficient Stratum Corneum: Characterization by Ruthenium Tetroxide Staining and X-Ray Diffraction. Journal of Investigative Dermatology, 1991, 96, 215-223.	0.3	284
4	An explanation for the rare occurrence of cis peptide units in proteins and polypeptides. Journal of Molecular Biology, 1976, 107, 85-92.	2.0	198
5	Three-dimensional structure of the nicotinic acetylcholine receptor and location of the major associated 43-kD cytoskeletal protein, determined at 22 A by low dose electron microscopy and x-ray diffraction to 12.5 A [published erratum appears in J Cell Biol 1989 Oct;109(4 Pt 1):1185]. Journal of Cell Biology, 1989, 109, 755-774.	2.3	115
6	The multifunctional histone-like protein Lsr2 protects mycobacteria against reactive oxygen intermediates. Proceedings of the National Academy of Sciences of the United States of America, 2009, 106, 4414-4418.	3.3	109
7	TORC1 organized in inhibited domains (TOROIDs) regulate TORC1 activity. Nature, 2017, 550, 265-269.	13.7	100
8	Dissecting the 3-D structure of vimentin intermediate filaments by cryo-electron tomography. Journal of Structural Biology, 2007, 158, 378-385.	1.3	80
9	Visualization of a water-selective pore by electron crystallography in vitreous ice. Proceedings of the National Academy of Sciences of the United States of America, 2001, 98, 1398-1403.	3.3	79
10	Three-dimensional fold of the human AQP1 water channel determined at 4 Ã resolution by electron crystallography of two-dimensional crystals embedded in ice 1 1Edited by W. Baumeister. Journal of Molecular Biology, 2000, 301, 369-387.	2.0	72
11	Volta phase plate cryo-EM of the small protein complex Prx3. Nature Communications, 2016, 7, 10534.	5.8	64
12	Three-dimensional Structure of the Toxin-delivery Particle Antifeeding Prophage of Serratia entomophila. Journal of Biological Chemistry, 2013, 288, 25276-25284.	1.6	57
13	Atomic structures of an entire contractile injection system in both the extended and contracted states. Nature Microbiology, 2019, 4, 1885-1894.	5.9	45
14	Membrane Remodeling by the Double-Barrel Scaffolding Protein of Poxvirus. PLoS Pathogens, 2011, 7, e1002239.	2.1	44
15	Peroxiredoxin is a Versatile Self-Assembling Tecton for Protein Nanotechnology. Biomacromolecules, 2014, 15, 1871-1881.	2.6	43
16	[7] Three-dimensional structure of membrane proteins determined by two-dimensional crystallization, electron cryomicroscopy, and image analysis. Methods in Enzymology, 1999, 294, 135-180.	0.4	40
17	Structures of Human Peroxiredoxin 3 Suggest Self-Chaperoning Assembly that Maintains Catalytic State. Structure, 2016, 24, 1120-1129.	1.6	39
18	Structure and function of kidney water channels. Kidney International, 1995, 48, 1069-1081.	2.6	38

#	Article	IF	CITATIONS
19	Wild-type and mutant bacteriorhodopsins D85N, D96N, and R82Q: purification to homogeneity, pH dependence of pumping and electron diffraction. Biochemistry, 1991, 30, 3088-3098.	1.2	37
20	The Structure of the Oligomerization Domain of Lsr2 from Mycobacterium tuberculosis Reveals a Mechanism for Chromosome Organization and Protection. PLoS ONE, 2012, 7, e38542.	1.1	37
21	Proton-Linked Dimerization of a Retroviral Capsid Protein Initiates Capsid Assembly. Structure, 2009, 17, 737-748.	1.6	33
22	Regulation and Quality Control of Adiponectin Assembly by Endoplasmic Reticulum Chaperone ERp44. Journal of Biological Chemistry, 2015, 290, 18111-18123.	1.6	33
23	Wild-type and mutant bacterioopsins D85N, D96N, and R82Q: high-level expression in Escherichia coli. Biochemistry, 1991, 30, 3082-3088.	1.2	32
24	A Structural Model for the Generation of Continuous Curvature on the Surface of a Retroviral Capsid. Journal of Molecular Biology, 2012, 417, 212-223.	2.0	32
25	Structural Polymorphism of Oligomeric Adiponectin Visualized by Electron Microscopy. Journal of Molecular Biology, 2008, 381, 419-430.	2.0	31
26	High sensitivity electron diffraction analysis. A study of divalent cation binding to purple membrane. Biophysical Journal, 1990, 57, 301-311.	0.2	30
27	Role of antifeeding prophage ( <scp>Afp</scp> ) protein <scp>Afp</scp> 16 in terminating the length of the <scp>Afp</scp> tailocin and stabilizing its sheath. Molecular Microbiology, 2013, 89, 702-714.	1.2	30
28	Cryo-Electron Microscopy Structure of Human Peroxiredoxin-3 Filament Reveals the Assembly of a Putative Chaperone. Structure, 2015, 23, 912-920.	1.6	30
29	Supine Orientation of a Murine MHC Class I Molecule on the Membrane Bilayer. Current Biology, 2004, 14, 718-724.	1.8	29
30	Large-Scale Structural Changes Accompany Binding of Lethal Factor to Anthrax Protective Antigen. Structure, 2004, 12, 2059-2066.	1.6	25
31	Proton-driven Assembly of the Rous Sarcoma Virus Capsid Protein Results in the Formation of Icosahedral Particles. Journal of Biological Chemistry, 2010, 285, 15056-15064.	1.6	24
32	Model of the toxic complex of anthrax: Responsive conformational changes in both the lethal factor and the protective antigen heptamer. Protein Science, 2006, 15, 2190-2200.	3.1	22
33	Visualization of biological macromolecules at near-atomic resolution: cryo-electron microscopy comes of age. Acta Crystallographica Section F, Structural Biology Communications, 2019, 75, 3-11.	0.4	22
34	Rapid Identification of Novel Inhibitors of the Human Aquaporinâ€1 Water Channel. Chemical Biology and Drug Design, 2016, 87, 794-805.	1.5	21
35	The Structure of a Putative Scaffolding Protein of Immature Poxvirus Particles as Determined by Electron Microscopy Suggests Similarity with Capsid Proteins of Large Icosahedral DNA Viruses. Journal of Virology, 2007, 81, 11075-11083.	1.5	19
36	Two-dimensional crystallization of Escherichia coli-expressed bacteriorhodopsin and its D96N variant: high resolution structural studies in projection. Biophysical Journal, 1993, 65, 1295-1306.	0.2	18

#	Article	IF	CITATIONS
37	Polymorphism in the Packing of Aquaporin-1 Tetramers in 2-D Crystals. Journal of Structural Biology, 2000, 130, 45-53.	1.3	18
38	Anthrax toxin-neutralizing antibody reconfigures the protective antigen heptamer into a supercomplex. Proceedings of the National Academy of Sciences of the United States of America, 2010, 107, 14070-14074.	3.3	16
39	Oligomeric Structure of Colicin Ia Channel in Lipid Bilayer Membranes. Journal of Biological Chemistry, 2009, 284, 16126-16134.	1.6	15
40	Synthetic peptides designed to modulate adiponectin assembly improve obesityâ€related metabolic disorders. British Journal of Pharmacology, 2017, 174, 4478-4492.	2.7	15
41	Structural Determinants of Rotavirus Subgroup Specificity Mapped by Cryo-electron Microscopy. Journal of Molecular Biology, 2006, 356, 209-221.	2.0	14
42	A peptide hydrogel derived from a fragment of human cardiac troponin C. Chemical Communications, 2016, 52, 4056-4059.	2.2	14
43	<scp>A</scp> fp14 is involved in regulating the length of Antiâ€feeding prophage ( <scp>A</scp> fp). Molecular Microbiology, 2015, 96, 815-826.	1.2	13
44	Multifunctional thermoresponsive designer peptide hydrogels. Acta Biomaterialia, 2017, 47, 40-49.	4.1	13
45	Expression, Purification, and Structural Characterization of the Bacteriorhodopsin–Aspartyl Transcarbamylase Fusion Protein. Protein Expression and Purification, 1999, 17, 324-338.	0.6	12
46	A PCR-directed cell-free approach to optimize protein expression using diverse fusion tags. Protein Expression and Purification, 2011, 80, 117-124.	0.6	12
47	Supramolecular Threading of Peptide Hydrogel Fibrils. ACS Biomaterials Science and Engineering, 2018, 4, 2733-2738.	2.6	12
48	A highly conserved tryptophan in the Nâ€ŧerminal variable domain regulates disulfide bond formation and oligomeric assembly of adiponectin. FEBS Journal, 2012, 279, 2495-2507.	2.2	10
49	Structural Model of the Tubular Assembly of the Rous Sarcoma Virus Capsid Protein. Journal of the American Chemical Society, 2017, 139, 2006-2013.	6.6	10
50	Stoichiometry and mechanistic implications of the MacAB-TolC tripartite efflux pump. Biochemical and Biophysical Research Communications, 2017, 494, 668-673.	1.0	10
51	Understanding the metal mediated assembly and hydrogel formation of a β-hairpin peptide. Biomaterials Science, 2017, 5, 1993-1997.	2.6	10
52	Aquaporins: Novel Targets for Age-Related Ocular Disorders. Journal of Ocular Pharmacology and Therapeutics, 2018, 34, 177-187.	0.6	10
53	Conformational flexibilities in malformin A. Biopolymers, 1984, 23, 2513-2524.	1.2	9
54	Structural Study of the <i>Serratia entomophila</i> Antifeeding Prophage: Three-Dimensional Structure of the Helical Sheath. Journal of Bacteriology, 2010, 192, 4522-4525.	1.0	8

#	Article	IF	CITATIONS
55	In vitro assembly of the Rous Sarcoma Virus capsid protein into hexamer tubes at physiological temperature. Scientific Reports, 2017, 7, 2913.	1.6	7
56	The Architecture of a Water-Selective Pore in the Lipid Bilayer Visualized by Electron Crystallography in Vitreous Ice. Novartis Foundation Symposium, 2008, , 33-50.	1.2	4
57	BACKBONE TORSIONAL POTENTIAL FUNCTIONS FOR ROTATIONS ABOUT Nâ€C <sub>α</sub> AND C <sub>α</sub> â€C BONDS IN DIPEPTIDE MODEL SYSTEMS IN RELATION TO NUCLEAR MAGNETIC RESONANCE AND INFRA RED SPECTRAL DATA*. International Journal of Peptide and Protein Research, 1978, 11, 166-178.	0.1	4
58	An investigation of the role of the adiponectin variable domain on the stability of the collagenâ€like domain. Biopolymers, 2014, 102, 313-321.	1.2	4
59			

#	Article	IF	CITATIONS
73	The architecture of a water-selective pore in the lipid bilayer visualized by electron crystallography in vitreous ice. Novartis Foundation Symposium, 2002, 245, 33-46; discussion 46-50; 165-8.	1.2	0